## **INORGANIC** CHEMISTRY







**FRONTIERS** 

## RESEARCH ARTICLE

View Article Online
View Journal | View Issue



**Cite this:** *Inorg. Chem. Front.*, 2022, **9**, 5688

# Decisive role of non-rare earth metals in high-regioselectivity addition of $\mu_3$ -carbido clusterfullerene†

Muqing Chen, \*\*\bigcup \*\frac{1}{2}a,b\* Yaoxiao Zhao, \frac{1}{2}c,f\* Fei Jin, \*b\* Mengyang Li, \*\bigcup c\* Runnan Guan, \*b\* Jinpeng Xin, \*b\* Yang-Rong Yao, \*b\* Xiang Zhao, \*\bigcup \*c\* Guan-Wu Wang, \*\bigcup \*d\* Qianyan Zhang, \*\bigcup \*e\* Su-Yuan Xie\* and Shangfeng Yang \*\bigcup \*b\*

Endohedral clusterfullerenes featuring encapsulation of metal clusters which transfer electrons to the outer fullerene cages show intriguing chemical properties different from empty fullerenes. Despite the extensive studies on the chemical properties of empty fullerenes, especially  $C_{60}$ , chemical functionalization of endohedral clusterfullerenes has been less explored, and previous reports are primarily limited to the well-known metal nitride and carbide clusterfullerenes. Herein, we report the first chemical functionalization of an emerging endohedral clusterfullerene  $\mu_3$ -carbido clusterfullerene (abbreviated as  $\mu_3$ -CCF) bearing central  $\mu_3$ -C and Ti(v) atoms forming a Ti=C double bond. A  $\mu_3$ -CCF Dy<sub>2</sub>TiC@ $I_p$ -C<sub>80</sub> is synthesized, and its molecular structure is unambiguously determined by single-crystal X-ray diffraction for the first time. A photochemical cycloaddition reaction of  $Dy_2TiC@I_h-C_{80}$  with 2-adamantane-2,3-[3H]-diazirine (abbreviated as AdN<sub>2</sub>) is then carried out and only one monoadduct  $Dy_2TiC@I_h-C_{80}$ -Ad is obtained, indicating its high regioselectivity. According to the X-ray single-crystal structure of Dy<sub>2</sub>TiC@I<sub>n</sub>-C<sub>80</sub>-Ad, the Ad moiety selectively attacks the [6,6]-bond (conjunction of two fused hexagons), which is adjacent to the Ti<sup>4+</sup> ion instead of the two  $Dy^{3+}$  ions, affording a [6,6]-open addition pattern. Theoretical calculations unveil that the Ti(w)ion plays a decisive role in high regioselectivity, and the formation of [6,6]-open Dy<sub>2</sub>TiC@I<sub>n</sub>-C<sub>80</sub>-Ad is thermodynamically preferred. Contrarily, a similar reaction of a Ti(III)-containing nitride clusterfullerene  $Y_2$ TiN@C<sub>80</sub> with AdN<sub>2</sub> is predicted to generate a different type of adduct with the addition sites adjacent to the  $Y^{3+}$  ion instead of the  $Ti^{3+}$  ion. This reveals the peculiarity of the chemical property of  $\mu_3$ -CCF resulting from the existence of the non-rare earth metal Ti with a high oxidation state.

Received 5th July 2022, Accepted 7th September 2022 DOI: 10.1039/d2qi01442d

rsc.li/frontiers-inorganic

<sup>a</sup>School of Environment and Civil Engineering, Dongguan University of Technology, Dongguan, Guangdong 523808, China. E-mail: mqchen@ustc.edu.cn <sup>b</sup>Hefei National Laboratory for Physical Sciences at Microscale, Key Laboratory of Materials for Energy Conversion, Chinese Academy of Sciences, Department of Materials Science and Engineering, Synergetic Innovation Center of Quantum Information & Quantum Physics, University of Science and Technology of China, Hefei 230026, China. E-mail: mqchen@ustc.edu.cn, sfyang@ustc.edu.cn <sup>c</sup>Institute of Molecular Science & Applied Chemistry, School of Chemistry, Xi'an Jiaotong University, Xi'an 710049, China. E-mail: xzhao@mail.xjtu.edu.cn <sup>d</sup>Hefei National Laboratory for Physical Sciences at Microscale, CAS Key Laboratory of Soft Matter Chemistry, and Department of Chemistry, University of Science and Technology of China, Hefei 230026, China. E-mail: gwang@ustc.edu.cn <sup>e</sup>State Key Lab for Physical Chemistry of Solid Surfaces, Collaborative Innovation Center of Chemistry for Energy Materials, Department of Chemistry, College of Chemistry and Chemical Engineering, Xiamen University, Xiamen 361005, China. E-mail: xmuzhangqy@xmu.edu.cn

<sup>f</sup>School of materials science and chemical engineering, Xi'an Technological University, Xi'an 710021, China

† Electronic supplementary information (ESI) available. CCDC 2036864 and 2036865. For ESI and crystallographic data in CIF or other electronic format see DOI: https://doi.org/10.1039/d2qi01442d

‡These authors contributed equally to this work.

#### Introduction

Chemical functionalization of fullerenes offers an opportunity to expand the properties and functionalities of the pristine fullerenes and is essential for applications of fullerene materials in versatile fields such as organic photovoltaic, biomedicine, and catalysis. 1-3 During the past three decades, extensive studies on the chemical properties of empty fullerenes, especially C60, have been reported. 4,5 Upon encapsulating metal clusters into fullerene cages, endohedral clusterfullerenes form and exhibit intriguing chemical properties different from empty fullerenes owing to electron transfer from the encapsulated metal cluster to the outer fullerene cage.6 Among the known clusterfullerenes, metal nitride and carbide clusterfullerenes were discovered first, and thus their chemical properties have been widely studied.<sup>7-9</sup> Up to now, several different types of chemical reactions, including [2 + 2]cycloadditions, 10,11 1,3-dipolar cycloaddition reactions, 12-14 disilylations, 15 Bingel-Hirsch reaction, 16,17 azide addition reac-

tions, 18 Lewis acid-base addition reactions, 19-21 carbene addition, 22-25 and radical reactions, 26,27 have been applied in functionalizing metal nitride and carbide clusterfullerenes. However, chemical functionalization of other types of endohedral clusterfullerenes has been less explored due mainly to their relatively low yield compared to the metal nitride clusterfullerenes (NCFs) such as Sc<sub>3</sub>N@C<sub>80</sub>.

As an emerging endohedral clusterfullerene, the µ<sub>2</sub>-carbido cluster-fullerene (abbreviated as µ3-CCF) discovered in 2014 appears quite special since a non-rare earth (RE) metal such as titanium (Ti) is needed, which bonds with a central  $\mu_3$ -C atom via a Ti=C double bond along with two RE metals.<sup>28</sup> So far, a few Ti-based μ<sub>3</sub>-CCFs have been isolated, including TiM<sub>2</sub>C@C<sub>80</sub>  $(M = Sc, Y, Nd, Gd, Tb, Dy, Er, and Lu)^{29-33}$  and  $TiSc_2C@C_{78}$ , the electronic configurations  $[Ti^{4+}(M^{3+})_2C^{4-}]^{6+}$   $@C_{2n}^{6-}$  involving a  $Ti^{4+}$  cation. Noteworthily, this is distinctly different from the conventional metal nitride clusterfullerenes (NCFs) M3N@C2n in which the encapsulated RE and non-RE metals take formal oxidation states of 3+, affording electronic configurations of  $[(M^{3+})_3N^{3-}]^{6+} @C_{2n}^{6-}.^{34-36}$ Thus, an open question arises: given that  $\mu_3$ -CCFs have similar trimetallic cluster compositions and the same charge state of the outer fullerene cage  $(C_{2n}^{6-})$  with NCFs, whether are their chemical properties similar to those of NCFs? However, to the best of our knowledge, the chemical functionalization of µ<sub>3</sub>-CCFs has never been reported yet, and hence their chemical properties, specifically, the impact of the encapsulated Ti<sup>4+</sup> cation, remain unknown.

Herein, we report the first chemical functionalization of µ<sub>3</sub>-CCF by a cycloaddition reaction of Dy<sub>2</sub>TiC@I<sub>h</sub>-C<sub>80</sub> with 2-adamantane-2,3-[3H]-diazirine (abbreviated as AdN2). Dy2TiC@Ih-C<sub>80</sub> is synthesized and its molecular structure is unambiguously determined by single-crystal X-ray diffraction for the first time. After a photochemical reaction of Dy<sub>2</sub>TiC@I<sub>h</sub>-C<sub>80</sub> with

AdN<sub>2</sub>, only one monoadduct Dy<sub>2</sub>TiC@I<sub>b</sub>-C<sub>80</sub>-Ad is obtained, indicating its high regioselectivity. On the basis of the X-ray single-crystal structure of Dy<sub>2</sub>TiC@I<sub>b</sub>-C<sub>80</sub>-Ad, a [6,6]-open addition pattern is identified. Theoretical calculations are carried out to unveil the role of the Ti<sup>4+</sup> ion within Dy<sub>2</sub>TiC@I<sub>h</sub>- $C_{80} \mu_3$ -CCF in its high regioselectivity.

#### Results and discussion

#### Synthesis, isolation and X-ray crystallographic structure of Dy<sub>2</sub>TiC@I<sub>h</sub>-C<sub>80</sub>

The synthesis procedure of  $Dy_2TiC@C_{80}$  by a modified Krätschmer-Huffman DC-arc discharge method is similar to that of Tb<sub>2</sub>TiC@C<sub>80</sub> we reported previously.<sup>32</sup> Isolation of Dy<sub>2</sub>TiC@I<sub>h</sub>-C<sub>80</sub> was fulfilled by a three-step high performance liquid chromatography (HPLC) procedure, and its high purity was confirmed by matrix-assisted laser desorption ionization time-of-flight (MALDI-TOF) mass spectroscopy and HPLC (see ESI Fig. S1†).

Although Dy<sub>2</sub>TiC@C<sub>80</sub> was reported by Popov et al. before, <sup>33</sup> its molecule structure has not been determined unambiguously yet. In this work, we succeeded in determining the molecular structure of Dy2TiC@C80 unambiguously by single-crystal X-ray diffraction for the first time on the basis of growing highquality cocrystals with decapyrrylcorannulene (DPC) as the host. The relative orientation of Dy<sub>2</sub>TiC@I<sub>h</sub>-C<sub>80</sub> and two DPC molecules within a 2DPC·{Dy2TiC@Ih-C80} cocrystal is shown in Fig. 1a, which includes only one orientation of the fullerene cage together with the major site of the Dy2TiC cluster for clarity (see ESI Table S1† for detailed crystallographic data). Similar to other reported clusterfullerene-DPC cocrystals, 37-39 the asymmetric crystal unit cell consists of one pair of fully ordered DPC molecules and one Dy2TiC@Ih-C80 molecule.

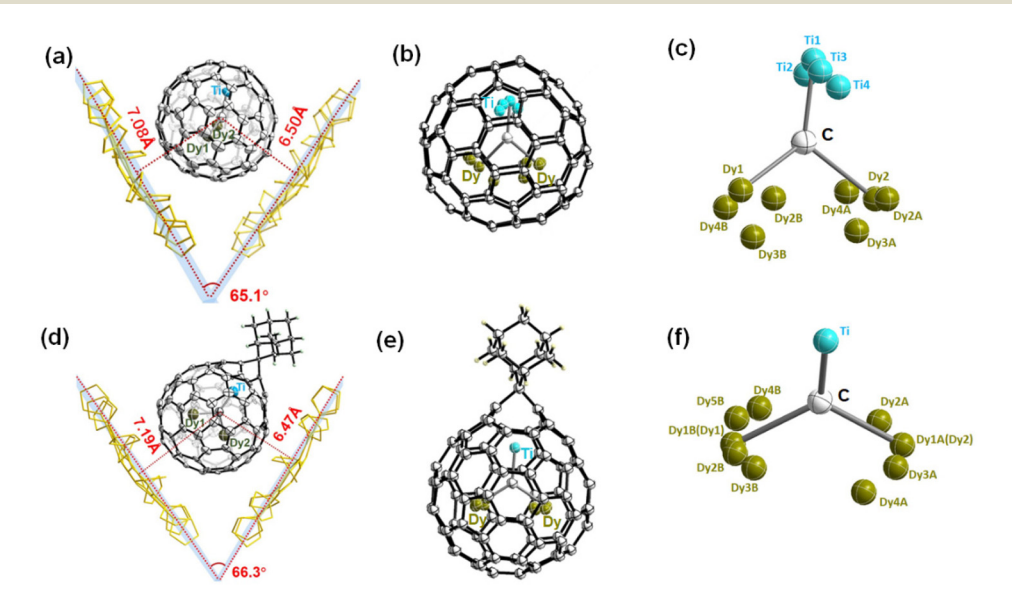


Fig. 1 Crystal structures of (a) 2DPC·{Dy<sub>2</sub>TiC@I<sub>h</sub>-C<sub>80</sub>} and (d) 2DPC·{Dy<sub>2</sub>TiC@I<sub>h</sub>-C<sub>80</sub>-Ad}. Geometric configurations of (b) Dy<sub>2</sub>TiC@I<sub>h</sub>-C<sub>80</sub> and (e)  $Dy_2TiC@I_n-C_{80}-Ad$  along with the metal positional disorder of the  $Dy_2TiC$  cluster within (c)  $Dy_2TiC@I_n-C_{80}$  and (f)  $Dy_2TiC@I_n-C_{80}-Ad$ .

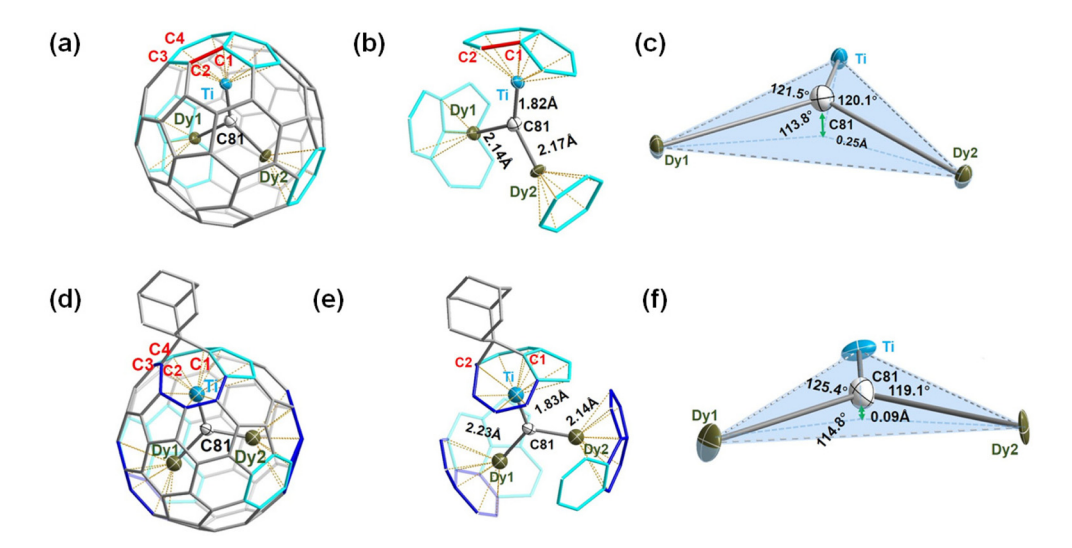


Fig. 2 The crystallographic orientation of the encapsulated Dy<sub>2</sub>TiC cluster inside (a and b) Dy<sub>2</sub>TiC@ $I_h$ -C<sub>80</sub> and (d and e) Dy<sub>2</sub>TiC@ $I_h$ -C<sub>80</sub>-Ad, as well as (c and f) the configurations of the Dy<sub>2</sub>TiC cluster inside both fullerene cages, are also shown. The blue and cyan regions indicate the coordination interactions between the encapsulated metals and the fullerene cage, and the C1-C2 bond is highlighted in red to show the difference before and after the Ad addition.

Meanwhile, two DPC molecules within 2DPC·{Dy₂TiC@I<sub>b</sub>-C<sub>80</sub>} exhibit a V-shape geometry with a dihedral angle of 65.1°, and the nearest DPC-C<sub>80</sub> cage center distances are 7.08 Å/6.50 Å, which is evidently different from that of 2DPC-{Sc<sub>3</sub>N@I<sub>h</sub>-C<sub>80</sub>} with a dihedral angle of 1.4° and a DPC-C80 cage center distance of 6.77/6.77 Å, 39 predicting the distinct electronic configuration of Dy<sub>2</sub>TiC@I<sub>h</sub>-C<sub>80</sub>, although they share the same I<sub>h</sub>symmetry C<sub>80</sub> cage.

The ordered  $I_b$ -C<sub>80</sub> cage and the major Dy/Ti sites with the largest occupancies (0.82, 0.91, and 0.80 for Dy1, Dy2, and Ti1, respectively) were extracted from the cocrystal for clarity (ESI Table S2†), showing that the Ti atom is located beneath a [5,6] bond, while the two Dy atoms are positioned beneath a hexagon and a [5,5,6] junction, respectively. Meanwhile, the shortest distances of the encapsulated metals and the outer cage carbons are 2.399 (9) Å, 2.344 (7) Å, and 2.132 (6) Å for Dy1-C75, Dy2-C11, and Ti-C42, respectively (ESI Table S3†), indicating strong metal-cage interactions which were verified by the high occupancy of two Dy atom and one Ti atom disorders. Furthermore, the bond length of Ti-C81 (1.824 (6) Å) is much shorter than those of Dy1-C81 (2.144(6) Å) and Dy2-C81 (2.175(6) Å) (Fig. 2b), indicating the existence of a Ti=C double bond as the characteristic of  $\mu_3\text{-CCF.}^{28,33}$  It is intriguing to investigate whether the encapsulated Dy2TiC cluster takes a planar or pyramidal configuration. We find that the sum value of ∠Dy1-C81-Ti, ∠Dy2-C81-Ti, and ∠Dy1-C81-Dy2 is 355.4° (Fig. 2c), indicating that the encapsulated Dy<sub>2</sub>TiC cluster is pyramidal, in which the C81 atom is 0.25 Å deviated from the plane composed of the TiDy<sub>2</sub> unit. This is similar to the case of Tb<sub>2</sub>TiC@C<sub>80</sub> but different from the planar cluster found in Lu<sub>2</sub>TiC@C<sub>80</sub>, in which the central carbon is 0.07 Å deviated from the trimetallic plane, 28 revealing the influence of the size of RE metal on the geometry of the M<sub>2</sub>TiC cluster.

#### Photochemical reactions of Dy<sub>2</sub>TiC@I<sub>b</sub>-C<sub>80</sub> with AdN<sub>2</sub>

Among the chemical functionalization methods developed for metal nitride and carbide clusterfullerenes, a cycloaddition reaction using AdN2 as a reagent has been demonstrated to exhibit high reactivity and regioselectivity. 22,24,25,40-43 Hence. in our present work we managed to investigate the cycloaddition reaction of Dy<sub>2</sub>TiC@I<sub>h</sub>-C<sub>80</sub> μ<sub>3</sub>-CCF with AdN<sub>2</sub>. The photochemical reaction of Dy<sub>2</sub>TiC@I<sub>h</sub>-C<sub>80</sub> with AdN<sub>2</sub> is shown in Fig. 3a. A mixture solution of Dy<sub>2</sub>TiC@I<sub>h</sub>-C<sub>80</sub> and excess AdN<sub>2</sub> in toluene was irradiated with a high-pressure mercury lamp, and the reaction process was monitored by analytical HPLC (Fig. 3b). Before the reaction, the HPLC profile of the pristine mixture solution showed two peaks at 3.6 and 39.8 min which were assigned to the AdN<sub>2</sub>/solvent peak and the pristine Dy<sub>2</sub>TiC@I<sub>h</sub>-C<sub>80</sub>, respectively. After light irradiation

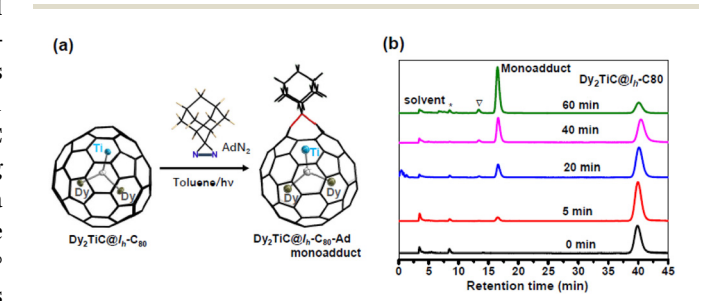


Fig. 3 (a) Synthetic route of Dy<sub>2</sub>TiC@I<sub>h</sub>-C<sub>80</sub>-Ad through the photochemical reaction of Dy<sub>2</sub>TiC@I<sub>h</sub>-C<sub>80</sub> with AdN<sub>2</sub>; (b) HPLC profiles of the reaction mixtures during the photochemical reaction process of  $Dy_2TiC@I_h-C_{80}$  with  $AdN_2$  with different reaction times. Conditions: Buckyprep column (Ø 4.6 mm × 250 mm), 20 μL injection volume, 1.0 mL min<sup>-1</sup> toluene flow. The inverted triangle and asterisk present the bisadduct and impurity, respectively.

for 5 min, a new peak appeared at 16.5 min, indicating the generation of the monoadduct Dy<sub>2</sub>TiC@I<sub>b</sub>-C<sub>80</sub>-Ad as confirmed by MALDI-TOF mass spectroscopic characterization. After prolonging the reaction time up to 60 min, the peak at 16.5 min continued to increase along with a decrease of the peak corresponding to the pristine Dy<sub>2</sub>TiC@I<sub>h</sub>-C<sub>80</sub>, indicating the promoted conversion of Dy<sub>2</sub>TiC@I<sub>h</sub>-C<sub>80</sub> to the monoadduct Dy<sub>2</sub>TiC@I<sub>h</sub>-C<sub>80</sub>-Ad. Finally, the reaction was stopped when an obvious peak of bisadduct at 13.3 min appears. Noteworthily, only one monoadduct Dy<sub>2</sub>TiC@I<sub>h</sub>-C<sub>80</sub>-Ad was obtained even after the reaction proceeded for 60 min, indicating its high regioselectivity. The resultant solution was then subjected to preparative HPLC separation, and the purity of Dy<sub>2</sub>TiC@I<sub>h</sub>-C<sub>80</sub>-Ad was verified by analytical HPLC (ESI Fig. S2a†). The purified Dy<sub>2</sub>TiC@I<sub>h</sub>-C<sub>80</sub>-Ad product was characterized by MALDI-TOF mass spectroscopy, showing an intense mass peak at m/z =1479.8 (ESI Fig. S2b†).

To identify the addition pattern of Dy<sub>2</sub>TiC@I<sub>h</sub>-C<sub>80</sub>-Ad, we grew high-quality cocrystals using DPC as the host similar to the case of the pristine Dy<sub>2</sub>TiC@I<sub>h</sub>-C<sub>80</sub>, and successfully determined the molecular structure of Dy2TiC@Ih-C80-Ad unambiguously by single-crystal X-ray diffraction. As illustrated in Fig. 1d, the asymmetric crystal unit cell of the 4DPC-2 {Dy2TiC@Ih-C80-Ad} cocrystal contains two pairs of fully ordered DPC molecules and two Dy<sub>2</sub>TiC@I<sub>h</sub>-C<sub>80</sub>-Ad molecules. DPC molecules within 2DPC-{Dy<sub>2</sub>TiC@I<sub>h</sub>-C<sub>80</sub>-Ad} exhibit a V-shape geometry with a dihedral angle of 66.3° similar to the pristine 2DPC·{Dy<sub>2</sub>TiC@I<sub>h</sub>-C<sub>80</sub>} cocrystal and the nearest DPC-C<sub>80</sub> cage center distances (7.19 Å/6.47 Å) exhibit only minor changes. However, different from the case of the pristine Dy<sub>2</sub>TiC@I<sub>h</sub>-C<sub>80</sub> with multiple position disorders of Dy and Ti atoms, the encapsulated Ti atom within Dy<sub>2</sub>TiC@I<sub>b</sub>-C<sub>80</sub>-Ad exhibits no positional disorders while the two Dy atoms still show several disorders (Fig. 1f, Table S2†). This indicates that the attachment of the Ad group between the C1-C2 bond which is fractured effectively traps the underneath Ti atom as a result of the strengthened Ti-cage interaction as discussed in detail below. Furthermore, the main occupancies of the endohedral two Dy atom disorder are 0.42 and 0.43 for Dy<sub>2</sub>TiC@I<sub>h</sub>-C<sub>80</sub>-Ad, which are obviously less than those (0.82 and 0.91) of pristine Dy<sub>2</sub>TiC@I<sub>h</sub>-C<sub>80</sub>, suggesting the weakened interaction of Dy atoms and the  $I_h$ -C<sub>80</sub> cage after carbene addition.

According to a close analysis of the single crystal structure of  $\mathrm{Dy_2TiC}@I_{\mathrm{h}}\text{-}\mathrm{C_{80}}\text{-}\mathrm{Ad}$ , the Ad moiety selectively attacks the [6,6]-bond (conjunction of two fused hexagons, C1–C2) which is adjacent to the  $\mathrm{Ti}^{4+}$  ion instead of the two  $\mathrm{Dy}^{3+}$  ions shown in Fig. 2d and e. Intriguingly, the distance (2.216(2) Å) of the addition sites (C1, C2) is much longer than that of the conventional C–C single bond (1.54 Å), indicating an open-cage addition pattern. <sup>22,41</sup> Hence, a [6,6]-open addition pattern of the Ad moiety can be deduced, which is similar to the cases of photochemical cycloaddition reactions of Ad with metal nitride and carbide clusterfullerenes. <sup>22,24,25,40</sup> Based on the largest occupancy, Dy1, Dy2, and Ti atoms within  $\mathrm{Dy_2TiC}@I_{\mathrm{h}}$ -C<sub>80</sub>-Ad locate underneath a [5,6] bond, a [5,6]-bond, and a fractured [6,6]-bond, respectively (Fig. 2d and e). It is obvious that

Ad addition leads to rotation of the Dy<sub>2</sub>TiC cluster from the coordinated blue region to the cyan region (see Fig. 2ab, d and e) due to the self-adaptive interaction between the endohedral cluster and the outer cage. For the encapsulated Dy2TiC cluster within Dy<sub>2</sub>TiC@I<sub>h</sub>-C<sub>80</sub>-Ad, the bond lengths of Dy1-C81 (2.242 (5) Å), Dy2-C81 (2.140(5) Å), and Ti-C81 (1.829 (5) Å) are close to those within the pristine Dy<sub>2</sub>TiC@I<sub>h</sub>-C<sub>80</sub> as discussed above (ESI Table S3 $\dagger$ ). These results indicate that the  $\mu_3$ -carbido nature of the encapsulated Dy2TiC cluster remains unchanged after grafting the Ad moiety. Moreover, the sum value of ∠Dy1-C81-Ti, ∠Dy2-C81-Ti and ∠Dy1-C81-Dy2 becomes 359.3° (Fig. 2f), which is larger than that observed for the pristine  $Dy_2TiC@I_h-C_{80}$  (355.4°), indicating that the cycloaddition of the Ad moiety to μ<sub>3</sub>-CCF induces an obvious geometric change of the encapsulated μ<sub>3</sub>-carbido cluster. A plausible explanation is that the grafted Ad moiety results in the deformation of the Ih-C80 cage with an enlargement of the confined internal space, and thus the strain of the Dy2TiC cluster is reduced. 22,24,25,40

#### Theoretical calculation of Dy2TiC@Ih-C80-Ad

To understand the high regioselectivity of Ad addition to  $Dy_2TiC@I_h$ - $C_{80}$   $\mu_3$ -CCF and unveil the role of the non-RE metal Ti within the  $\mu_3$ -carbido cluster, we performed comprehensive theoretical studies. Density functional theory (DFT) computations on the pristine  $Dy_2TiC@I_h$ - $C_{80}$   $\mu_3$ -CCF with S=5 spin ground state (spin multiple state 2S+1=11) were carried out, verifying that the encapsulated  $Dy_2TiC$  cluster takes a  $\mu_3$ -carbido structure bearing a  $Ti^{4+}$  ion and Ti—C double bond (1.79 Å) (ESI Tables S4–S5, Fig. S3–S4†). Besides, the electronic configuration of  $[(Dy^{3+})_2Ti^{4+}C^{4-}]^{6+}@[I_h(31924)-C_{80}]^{6-}$  is confirmed similar to the case of the first  $\mu_3$ -CCF  $Lu_2TiC@I_h$ - $C_{80}$ .

The high regioselectivity of Ad addition around Ti instead of Dy can be understood by further analyzing the geometric and electronic configuration of  $\mathrm{Dy_2TiC}@I_{\mathrm{h}}\text{-}\mathrm{C}_{80}$ . First, the shorter Ti–C (cage) distances than those of Dy–C (cage) suggest much stronger interactions between  $\mathrm{Ti}^{4+}$  with the  $I_{\mathrm{h}}$ -C<sub>80</sub> cage (ESI Table S6†), which is also confirmed by the larger Mayer bond order (MBO), density of electrons, and the Laplacian of the electron density between the  $\mathrm{Ti}^{4+}$  ion and the  $I_{\mathrm{h}}$ -C<sub>80</sub> cage than those of  $\mathrm{Dy}^{3+}$  ions with the  $I_{\mathrm{h}}$ -C<sub>80</sub> cage (ESI Tables S6 and S7†). Besides, the  $\mathrm{Ti}^{4+}$  ion and its adjacent cage carbons with much more negative charges also contribute to the stronger interactions of  $\mathrm{Ti}^{4+}$ -C (cage) than that of  $\mathrm{Dy}^{3+}$ -C (cage) (ESI Fig. S4d†).

Considering the simultaneously appeared [5,6]-adduct and [6,6]-adduct isomers in the reaction of  $M_3N@I_h\text{-}C_{80}$  (M = Sc, Lu) with carbene Ad: under light irradiation, <sup>22</sup> it is interesting that our experimental finding shows that only [6,6]-adduct around the  $\text{Ti}^{4+}$  ion obtained with C1 and C2 as the addition sites instead of C2 and C3 ([5,6]-adduct isomer). The theoretical calculations indicate that the [6,6]-adduct has 3.3 kcal  $\text{mol}^{-1}$  potential energy (Fig. 4) lower than the [5,6]-adduct. Furthermore, statistical thermodynamic analysis considering the entropy–enthalpy effect shows that [6,6]-open  $\text{Dy}_2\text{TiC}@I_h\text{-}C_{80}\text{-Ad}$  (C1, C2) has the 99.97% distribution relative to that

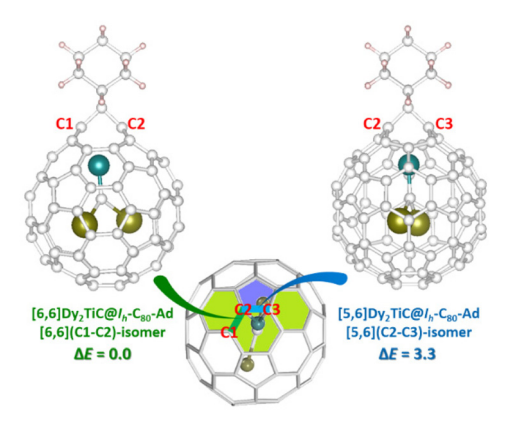


Fig. 4 Relative energies ( $\Delta E$ , in kcal mol<sup>-1</sup>) of [5,6]-Dy<sub>2</sub>TiC@ $I_h$ -C<sub>80</sub>-Ad (in blue) and [6,6]-Dy<sub>2</sub>TiC@ $I_h$ -C<sub>80</sub>-Ad (in green). The cyan, brown, and light gray balls represent the titanium, dysprosium and carbon atoms, respectively.

(0.03%) of [5,6]-open Dy<sub>2</sub>TiC@ $I_h$ -C<sub>80</sub>-Ad (C2-C3) at 298.15 K. Thus, the [6,6]-open Dy<sub>2</sub>TiC@ $I_h$ -C<sub>80</sub>-Ad obtained in experiment is the thermodynamic product, which is the same as the reactions of AdN2 with several endohedral metallofullerenes previously reported. 23,43

In order to consolidate the universal role of the Ti(IV) within the μ<sub>3</sub>-carbido cluster in determining the regioselectivity and reaction mechanism of µ3-CCF, we further computed similar cycloaddition products of the analogously reported  $\mu_3$ -CCF  $Y_2$ TiC@ $I_h$ -C $_{80}$   $^{33}$  and nitride clusterfullerene  $Y_2$ TiN@C $_{80}$  bearing Ti(III) $^{44,45}$  with AdN $_2$ , in which replacing  $Dy^{3+}$  with  $Y^{3+}$  is to ensure the validity of  $\mu_3$ -CCF clusterfullerenes. Fig. 5 shows that without the presence of Ti(IV), the Ad moiety of Ti(III)-based [6,6]-Y2TiN@Ih-C80-Ad with the lowest potential energy is located nearly around the Y atom. However, similar to Dy<sub>2</sub>TiC@I<sub>h</sub>-C<sub>80</sub>-Ad, the Ad moiety selectively attacks the [6,6]-bond of  $I_h$ -C<sub>80</sub> adjacent to the Ti(IV) instead of the Y atom to form a Y<sub>2</sub>TiC@I<sub>h</sub>-C<sub>80</sub>-Ad adduct with energy superiority. Further frontier molecular orbital (FMO) computations in Fig. S6† show that in the presence of Ti(IV), the FMO occupancy of Dy<sub>2</sub>TiC@I<sub>h</sub>-C<sub>80</sub> and Y<sub>2</sub>TiC@I<sub>h</sub>-C<sub>80</sub> are similar to each other (ESI Fig. S5†), but different to that of  $Y_2 \text{TiN} @ I_h - C_{80}$  bearing Ti(III). This reveals the decisive role of the Ti<sup>4+</sup> ion with a high formal oxidation state (IV) in the electronic configuration of μ<sub>3</sub>-CCF M<sub>2</sub>TiC@I<sub>h</sub>-C<sub>80</sub>, which directly affects the reactivity. Thus, the cycloaddition reaction of Y<sub>2</sub>TiC@I<sub>h</sub>-C<sub>80</sub> with AdN<sub>2</sub> is expected to exhibit similar regioselectivity and addition pattern to that of  $\mathrm{Dy_2TiC}@I_{\mathrm{h}}\text{-}\mathrm{C}_{80}.$ 

#### Effect of Ad addition on the electronic properties of Dy<sub>2</sub>TiC@I<sub>h</sub>-C<sub>80</sub>

In order to unveil the effect of Ad addition on the electronic properties of Dy<sub>2</sub>TiC@I<sub>h</sub>-C<sub>80</sub>, we carried out UV-vis-NIR spectroscopic characterization and electrochemical studies (Fig. 6). Their characteristic absorption data and redox potentials along with those of other analogous clusterfullerenes are sum-

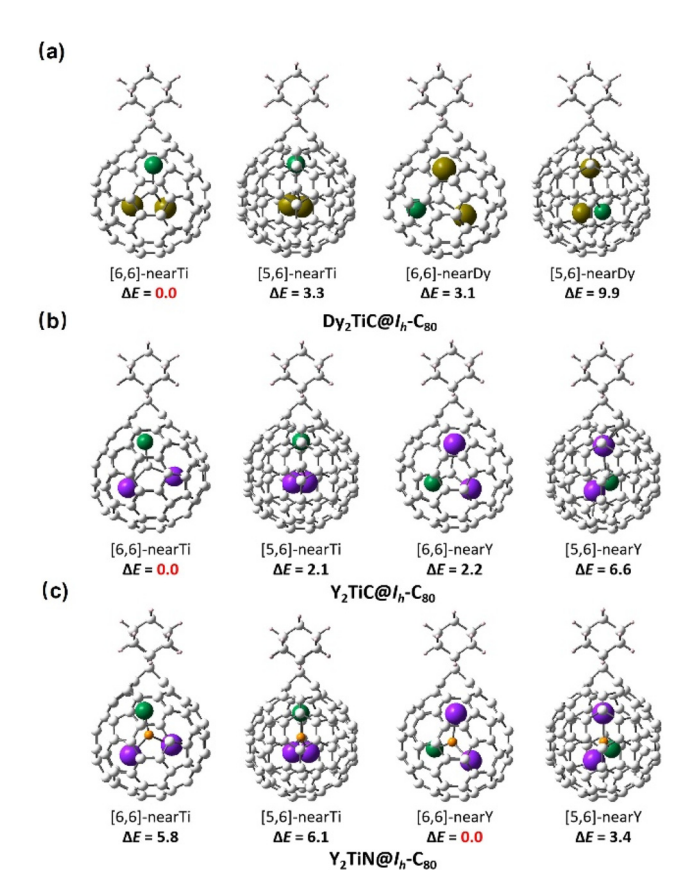


Fig. 5 Relative energies ( $\Delta E$ , in kcal mol<sup>-1</sup>) of Dy<sub>2</sub>TiC@ $I_h$ -C<sub>80</sub> (a),  $Y_2TiC@I_h-C_{80}$  (b) and  $Y_2TiN@I_h-C_{80}$  (c) with different addition sites of Ad. The green, brown, purple and light gray balls represent the titanium, dysprosium, yttrium and carbon atoms, respectively.

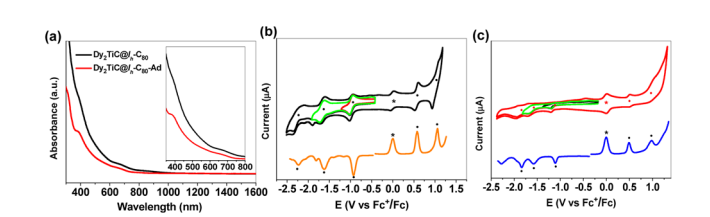


Fig. 6 (a) UV-vis-NIR spectra of Dy<sub>2</sub>TiC@I<sub>h</sub>-C<sub>80</sub> and Dy<sub>2</sub>TiC@I<sub>h</sub>-C<sub>80</sub>-Ad dissolved in toluene. Inset: Enlarged spectral region of 350-800 nm. Cyclic voltammograms of (b)  $Dy_2TiC@I_h-C_{80}$  and (c)  $Dy_2TiC@I_h-C_{80}-Ad$ in 1,2-dichlorobenzene solution with ferrocene (Fc) as the internal standard under a nitrogen atmosphere. Scan rate: 100 mV s<sup>-1</sup>, tetrabutylammonium hexafluorophosphate (TBAPF<sub>6</sub>) as the supporting electrolyte. Each redox step is marked with a solid dot to aid comparison; the asterisk denotes the oxidation peak of ferrocene.

marized (ESI Table S8†). The absorption spectrum of Dy<sub>2</sub>TiC@I<sub>h</sub>-C<sub>80</sub> in the range of 300-1600 nm is featureless, with two broad shoulder peaks at 390 and 676 nm. After grafting an Ad moiety, the shoulder peak at 390 nm becomes more apparent in the absorption spectrum of Dy<sub>2</sub>TiC@I<sub>h</sub>-C<sub>80</sub>-Ad (Fig. 6a) and the shoulder peak at 676 nm exhibits a negligible change. These results indicate that Ad addition induces little influence on the optical absorption of  $Dy_2TiC@I_h-C_{80}$ .

Cyclic voltammometry (CV) and differential pulse voltammetry (DPV) of the pristine Dy<sub>2</sub>TiC@I<sub>h</sub>-C<sub>80</sub> and Dy<sub>2</sub>TiC@I<sub>h</sub>-C<sub>80</sub>-Ad are then compared as illustrated in Fig. 6b and c. The pristine Dy<sub>2</sub>TiC@I<sub>h</sub>-C<sub>80</sub> exhibits two reversible reduction steps, one irreversible reduction step and two reversible oxidation steps which are similar to those reported by Popov et al. 33 After Ad addition, all three reduction steps become irreversible, and the first reduction potential shifts negatively from -0.93 V (half-wave potential) to -1.10 V (peak potential), whereas the second and third reduction potentials exhibit a negligible cathodical shift. Only one reversible oxidation step and one irreversible oxidation peak are observed for Dy<sub>2</sub>TiC@I<sub>h</sub>-C<sub>80</sub>-Ad, with the first oxidation potential cathodically shifting from 0.57 V to 0.49 V relative to that of the pristine Dy<sub>2</sub>TiC@I<sub>h</sub>-C<sub>80</sub> (ESI Table S8†). This cathodical shift of redox potentials in Dy2TiC@Ih-C80 after carbene functionalization is similar to those of Ad adducts of M3N@C80 (M = Sc, Lu) reported previously.<sup>22</sup>

## Conclusion

In summary, the first chemical functionalization of μ<sub>3</sub>-CCF exemplified by Dy<sub>2</sub>TiC@I<sub>h</sub>-C<sub>80</sub> is studied, revealing the decisive role of the non-rare earth metal Ti(IV) in high-regioselectivity addition. The molecular structure of the pristine Dy<sub>2</sub>TiC@I<sub>h</sub>-C<sub>80</sub> is unambiguously determined by single-crystal X-ray diffraction for the first time, revealing the feature of the Ti=C double bond and the influence of the size of rare earth metals on the geometry of the M2TiC cluster. A photochemical cycloaddition reaction of Dy2TiC@Ih-C80 with I2 affords only one monoadduct Dy2TiC@Ih-C80-Ad, indicating its high regioselectivity. On the basis of the X-ray single crystal structure of Dy<sub>2</sub>TiC@I<sub>h</sub>-C<sub>80</sub>-Ad, the Ad moiety selectively attacks the [6,6]bond which is adjacent to the Ti<sup>4+</sup> ion instead of the two Dy<sup>3+</sup> ions, and the presence of a [6,6]-open addition pattern is confirmed. According to theoretical calculations, Dy<sub>2</sub>TiC@I<sub>h</sub>-C<sub>80</sub>-Ad is thermodynamically preferred, and the Ti(IV) ion plays a decisive role in high regioselectivity. In contrast, a similar reaction of a Ti(III)-containing nitride clusterfullerene Y2TiN@C80 with AdN<sub>2</sub> is predicted theoretically to generate a different type of adduct with the addition site adjacent to the Y<sup>3+</sup> ion instead of the Ti<sup>3+</sup> ion. Hence, the peculiarity of the chemical properties of µ<sub>3</sub>-CCF resulting from the existence of the non-rare earth metal Ti with a high oxidation state is unveiled. As the first chemical functionalization of μ<sub>3</sub>-carbido clusterfullerene with high regioselectivity, our finding on the decisive role of non-rare earth metal titanium in the regioselectivity fulfills an in-depth understanding of the fascinating chemical properties of endohedral fullerenes.

## **Experimental**

#### **Detailed experimental process**

A toluene solution (25 mL) containing approximately 5 mg of Dy<sub>2</sub>TiC@I<sub>h</sub>-C<sub>80</sub> and excessive AdN<sub>2</sub> was first degassed for

about 15 minutes and later was irradiated with a high-pressure mercury-arc lamp (cutoff <350 nm) at room temperature. The reaction process was monitored by analytical HPLC. The detailed separation procedure of monoadduct Dy2TiC@Ih-C80-Ad using preparative HPLC is presented in the ESI† (LC-908 instrument, Japan Analytical Industry Co., Ltd, toluene as the mobile phase). MALDI-TOF MS was performed on a BIFLEX III (Bruker, Germany) with 1,1,4,4-tetraphenyl-1,3-butadiene (TPB) as the matrix.

#### Spectroscopic and electrochemical studies

UV-Vis-NIR spectra were recorded on a UV 3150 (Shimadzu, Japan) in toluene. Cyclic voltammetry (CV) and differential pulse voltammetry (DPV) were obtained in 1,2-dichlorobenzene with 0.1 M (n-Bu)<sub>4</sub>NPF<sub>6</sub> as the supporting electrolyte using a CHI660E workstation. Pt disc, Pt wire and silver wire were used as the working electrode, reference electrode and auxiliary electrode, respectively. The scan rate for CV was 20 mV s<sup>-1</sup>. Conditions for DPV: pulse amplitude, 50 mV; scan rate,  $20 \text{ mV s}^{-1}$ .

#### X-ray crystallographic study

Crystal blocks of Dy<sub>2</sub>TiC@I<sub>h</sub>-C<sub>80</sub> and Dy<sub>2</sub>TiC@I<sub>h</sub>-C<sub>80</sub>-Ad were obtained by slow volatilization of a toluene solution of DPC and Dy<sub>2</sub>TiC@I<sub>h</sub>-C<sub>80</sub>/Dy<sub>2</sub>TiC@I<sub>h</sub>-C<sub>80</sub>-Ad in a glass tube. After two weeks, black block crystals suitable for crystal measurements were formed. Single-crystal XRD measurements of Dy<sub>2</sub>TiC@I<sub>h</sub>-C<sub>80</sub> and Dy<sub>2</sub>TiC@I<sub>h</sub>-C<sub>80</sub>-Ad crystals were conducted at 100 K at the BL17B station of Shanghai Synchrotron Radiation Facility. The crystal structures were solved with the ShelXT structure solution program using the Intrinsic Phasing method, later refined with the ShelXL<sup>46</sup> refinement package embedded within OLEX2.47 CCDC 2036864 and 2036865† contain the supplementary crystallographic data for Dy<sub>2</sub>TiC@I<sub>h</sub>-C<sub>80</sub> and Dy<sub>2</sub>TiC@I<sub>h</sub>-C<sub>80</sub>-Ad, respectively.

## **Author contributions**

M. C. and Y. Z. contributed equally to this work. M. C. performed the chemical reaction of Dy2TiC@C80 with AdN2 and confirmed the crystal structures of Dy<sub>2</sub>TiC@C<sub>80</sub> and Dy<sub>2</sub>TiC@C<sub>80</sub>-Ad by the crystal growth, crystal measurements and resolution. Meanwhile, M. C. wrote the original draft. Y. Z., M. L. and X. Z. carried out the theoretical calculation and analysis of Dy<sub>2</sub>TiC@C<sub>80</sub> and Dy<sub>2</sub>TiC@C<sub>80</sub>-Ad. F. J., J. X. and R. G. synthesized and separated Dy<sub>2</sub>TiC@C<sub>80</sub> for crystal growth and further chemical functionalization. Q. Z. provided decapyrrylcorannulene (DPC) which was used as the host to obtain high-quality single crystals of Dy<sub>2</sub>TiC@C<sub>80</sub> and Dy<sub>2</sub>TiC@C<sub>80</sub>-Ad. S. X., G. W. and S. Y. provided the discussion and article revision.

#### Conflicts of interest

The authors declare no competing financial interest.

## Acknowledgements

This work was partially supported by the National Key Research and Development Program China (2017YFA0402800) and the National Natural Science Foundation of China (52172053, 51925206, 21772189, U1932214, 21773181, 21573172 and 91961113). We thank the staff from BL17B1 at Shanghai Synchrotron Radiation Facility for assistance during data collection. We thank the staff from the BL17B1beamline of the National Facility for Protein Science in Shanghai (NFPS) at Shanghai Synchrotron Radiation Facility, for assistance during data collection.

#### References

- R. B. Ross, C. M. Cardona, D. M. Guldi,
   S. G. Sankaranarayanan, M. O. Reese, N. Kopidakis, J. Peet,
   B. Walker, G. C. Bazan, E. Van Keuren, B. C. Holloway and
   M. Drees, Endohedral fullerenes for organic photovoltaic devices, *Nat. Mater.*, 2009, 8, 208–212.
- 2 J. Tang, R. Zhang, M. Guo, H. Zhou, Y. Zhao, Y. Liu, Y. Wu and C. Chen, Gd-metallofullerenol drug delivery system mediated macrophage polarization enhances the efficiency of chemotherapy, *J. Controlled Release*, 2020, 320, 293–303.
- 3 A. R. Puente Santiago, O. Fernandez-Delgado, A. Gomez, M. A. Ahsan and L. Echegoyen, Fullerenes as Key Components for Low-Dimensional (Photo)electrocatalytic Nanohybrid Materials, *Angew. Chem., Int. Ed.*, 2021, **60**, 122–141.
- 4 M. D. Tzirakis and M. Orfanopoulos, Radical Reactions of Fullerenes: From Synthetic Organic Chem-istry to Materials Science and Biology, *Chem. Rev.*, 2013, **113**, 5262–5321.
- 5 M. Yamada, T. Akasaka and S. Nagase, Carbene Additions to Fullerenes, *Chem. Rev.*, 2013, 113, 7209–7264.
- 6 S. Yang, T. Wei and F. Jin, When metal clusters meet carbon cages: endohedral clusterfullerenes, *Chem. Soc. Rev.*, 2017, **46**, 5005–5058.
- 7 P. Jin, Y. Li, S. Magagula and Z. Chen, Exohedral functionalization of endohedral metallofullerenes: Interplay between inside and outside, *Coord. Chem. Rev.*, 2019, **388**, 406–439.
- 8 M. N. Chaur, F. Melin, A. L. Ortiz and L. Echegoyen, Chemical, electrochemical, and structural properties of endohedral metallofullerenes, *Angew. Chem., Int. Ed.*, 2009, 48, 7514–7538.
- 9 X. Lu, L. Feng, T. Akasaka and S. Nagase, Current status and future developments of endohedral metallofullerenes, *Chem. Soc. Rev.*, 2012, **41**, 7723–7760.
- 10 F.-F. Li, J. R. Pinzon, B. Q. Mercado, M. M. Olmstead, A. L. Balch and L. Echegoyen, [2+2] Cycloaddition Reaction

- to  $Sc_3N@I_h$ ,- $C_{80}$ . The Formation of Very Stable [5,6]- and [6,6]-Adducts, *J. Am. Chem. Soc.*, 2011, **133**, 1563–1571.
- 11 G.-W. Wang, T.-X. Liu, M. Jiao, N. Wang, S.- E. Zhu, C. Chen, S. Yang, F. L. Bowles, C. M. Beavers, M. M. Olmstead, B. Q. Mercado and A. L. Balch, The cycloaddition reaction of I(h)-Sc3N@C80 with 2-amino-4,5-diiso-propoxybenzoic acid and isoamyl nitrite to produce an open-cage metallofullerene, *Angew. Chem., Int. Ed.*, 2011, 50, 4658–4662.
- 12 C. M. Cardona, A. Kitaygorodskiy, A. Ortiz, M. A. Herranz and L. Echegoyen, The first fulleropyrrolidine derivative of Sc<sub>3</sub>N@C<sub>80</sub>: pronounced chemical shift differences of the geminal protons on the pyrrolidine ring, *J. Org. Chem.*, 2005, **70**, 5092–5097.
- 13 M. Chen, R. Guan, B. Li, L. Yang, C. Niu, P. Jin, G.-W. Wang and S. Yang, Anomalous Cis-Conformation Regioselectivity of Heterocycle-Fused Sc<sub>3</sub>N@D<sub>3h</sub>,-C<sub>78</sub> Derivatives, *Angew. Chem., Int. Ed.*, 2021, 60, 7880–7886.
- 14 O. Semivrazhskaya, A. Romero-Rivera, S. Aroua, S. I. Troyanov, M. Garcia-Borras, S. Stevenson, S. Osuna and Y. Yamakoshi, Structures of Gd<sub>3</sub>N@C<sub>80</sub> Prato Bis-Adducts: Crystal Structure, Thermal Isomerization, and Computational Study, *J. Am. Chem. Soc.*, 2019, 141, 10988–10993.
- 15 T. Wakahara, Y. Iiduka, O. Ikenaga, T. Nakahodo, A. Sakuraba, T. Tsuchiya, Y. Maeda, M. Kako, T. Akasaka, K. Yoza, E. Horn, N. Mizorogi and S. Nagase, Characterization of the bis-silylated endofullerene Sc<sub>3</sub>N@C<sub>80</sub>, J. Am. Chem. Soc., 2006, 128, 9919–9925.
- 16 Y. Hu, A. Sole-Daura, Y.-R. Yao, X. Liu, S. Liu, A. Yu, P. Peng, J. M. Poblet, A. Rodriguez-Fortea, L. Echegoyen and F.-F. Li, Chemical Reactions of Cationic Metallofullerenes: An Alternative Route for Exohedral Functionalization, *Chem. Eur. J.*, 2020, 26, 1748–1753.
- 17 T. Cai, L. Xu, C. Shu, H. A. Champion, J. E. Reid, C. Anklin, M. R. Anderson, H. W. Gibson and H. C. Dorn, Selective formation of a symmetric Sc<sub>3</sub>N@C<sub>78</sub> bisadduct: Adduct docking controlled by an internal trimetallic nitride cluster, *J. Am. Chem. Soc.*, 2008, 130, 2136–2137.
- 18 T.-X. Liu, T. Wei, S.-E. Zhu, G.-W. Wang, M. Jiao, S. Yang, F. L. Bowles, M. M. Olmstead and A. L. Balch, Azide Addition to an Endohedral Metallofullerene: Formation of Azafulleroids of Sc<sub>3</sub>N@I<sub>h</sub>-C<sub>80</sub>, J. Am. Chem. Soc., 2012, 134, 11956–11959.
- 19 M. Chen, L. Bao, M. Ai, W. Shen and X. Lu, Sc<sub>3</sub>N@*I<sub>h</sub>*,-C<sub>80</sub> as a novel Lewis acid to trap abnormal N-heterocyclic carbenes: the unprecedented formation of a singly bonded [6,6,6]-adduct, *Chem. Sci.*, 2016, 7, 2331–2334.
- 20 M. Chen, W. Shen, P. Peng, L. Bao, S. Zhao, Y. Xie, P. Jin, H. Fang, F.-F. Li and X. Lu, Evidence of Oxygen Activation in the Reaction between an N-Heterocyclic Carbene and  $M_3N@I_h(7)$ - $C_{80}$ : An Unexpected Method of Steric Hindrance Release, *J. Org. Chem.*, 2017, **82**, 3500–3505.
- 21 L. Bao, M. Chen, W. Shen, L. Yang, P. Jin and X. Lu, Lewis Acid-Base Adducts of Sc<sub>2</sub>C<sub>2</sub>@C<sub>3v</sub>(8)-C<sub>82</sub>/N-Heterocyclic Carbene: Toward Isomerically Pure Metallofullerene Derivatives, *Inorg. Chem.*, 2017, **56**, 14747–14750.

- 22 M. Yamada, T. Abe, C. Saito, T. Yamazaki, S. Sato, N. Mizorogi, Z. Slanina, F. Uhlik, M. Suzuki, Y. Maeda, Y. Lian, X. Lu, M. M. Olmstead, A. L. Balch, S. Nagase and T. Akasaka, Adamantylidene Addition to M<sub>3</sub>N@I<sub>h</sub>-C<sub>80</sub> (M=Sc, Lu) and Sc3N@D5h,-C80: Synthesis Crystallographic Characterization of the [5,6]-Open and [6,6]-Open Adducts, Chem. - Eur. J., 2017, 23, 6552-6561.
- 23 M. Yamada, Y. Tanabe, J. Dang, S. Sato, N. Mizorogi, M. Hachiya, M. Suzuki, T. Abe, H. Kurihara, Y. Maeda, X. Zhao, Y. Lian, S. Nagase and T. Akasaka,  $D_{2d}$ , (23)-C<sub>84</sub> versus Sc<sub>2</sub>C<sub>2</sub>@D<sub>2d</sub>(23)-C<sub>84</sub>: Impact of Endohedral Sc<sub>2</sub>C<sub>2</sub> Doping on Chemical Reactivity in the Photolysis of Diazirine, J. Am. Chem. Soc., 2016, 138, 16523-16532.
- 24 Y. Iiduka, T. Wakahara, T. Nakahodo, T. Tsuchiya, A. Sakuraba, Y. Maeda, T. Akasaka, K. Yoza, E. Horn, T. Kato, M. T. H. Liu, N. Mizorogi, K. Kobayashi and S. Nagase, Structural determination of metallofullerene Sc<sub>3</sub>C<sub>82</sub> revisited: a surprising finding, J. Am. Chem. Soc., 2005, 127, 12500-12501.
- 25 Y. Iiduka, T. Wakahara, K. Nakajima, T. Nakahodo, T. Tsuchiya, Y. Maeda, T. Akasaka, K. Yoza, M. T. H. Liu, N. Mizorogi and S. Nagase, Experimental and theoretical studies of the scandium carbide endohedral metallofullerene Sc<sub>2</sub>C<sub>2</sub>@C<sub>82</sub> and its carbene derivative, Angew. Chem., Int. Ed., 2007, 46, 5562-5564.
- 26 C. Shu, C. Slebodnick, L. Xu, H. Champion, T. Fuhrer, T. Cai, J. E. Reid, W. Fu, K. Harich, H. C. Dorn and H. W. Gibson, Highly Regioselective Derivatization of Trimetallic Nitride Templated Endohedral Metallofullerenes via a Facile Photochemical Reaction, J. Am. Chem. Soc., 2008, 130, 17755-17760.
- 27 N. B. Shustova, A. A. Popov, M. A. Mackey, C. E. Coumbe, J. P. Phillips, S. Stevenson, S. H. Strauss and O. V. Boltalina, Radical trifluoromethylation of Sc<sub>3</sub>N@C<sub>80</sub>, J. Am. Chem. Soc., 2007, 129, 11676-11677.
- 28 A. L. Svitova, K. B. Ghiassi, C. Schlesier, K. Junghans, Y. Zhang, M. M. Olmstead, A. L. Balch, L. Dunsch and A. A. Popov, Endohedral fullerene with μ3-carbido ligand and titanium-carbon double bond stabilized inside a carbon cage, Nat. Commun., 2014, 5, 3568.
- 29 K. Junghans, K. B. Ghiassi, N. A. Samoylova, Q. Deng, M. Rosenkranz, M. M. Olmstead, A. L. Balch and A. A. Popov, Synthesis and Isolation of the Titanium-Endohedral Fullerenes- $Sc_2TiC@I_h$ ,- $C_{80}$ , Scandium Sc2TiC@D5h-C80 and Sc2TiC2@Ih-C80: Metal Size Tuning of the Ti(IV)/Ti(III) Redox Potentials, Chem. - Eur. J., 2016, 22, 13098-13107.
- 30 C. Fuertes-Espinosa, A. Gomez-Torres, R. Morales-Martinez, A. Rodriguez-Fortea, C. Garcia-Simon, F. Gandara, I. Imaz, J. Juanhuix, D. Maspoch, J. M. Poblet, L. Echegoyen and X. Ribas, Purification of Uranium-based Endohedral Metallofullerenes (EMFs) by Selective Supramolecular Encapsulation and Release, Angew. Chem., Int. Ed., 2018, 57, 11294-11299.
- 31 A. Brandenburg, D. S. Krylov, A. Beger, A. U. B. Wolter, B. Buchner and A. A. Popov, Carbide clusterfullerene

- DyYTiC@C<sub>80</sub> featuring three different metals in the endohedral cluster and its single-ion magnetism, Chem. Commun., 2018, 54, 10683-10686.
- 32 F. Liu, F. Jin, S. Wang, A. A. Popov and S. Yang, Pyramidal TiTb<sub>2</sub>C cluster encapsulated within the popular  $I_h(7)$ -C<sub>80</sub> fullerene cage, Inorg. Chim. Acta, 2017, 468, 203-208.
- 33 K. Junghans, C. Schlesier, A. Kostanyan, N. A. Samoylova, Q. M. Deng, M. Rosenkranz, S. Schiemenz, R. Westerstrom, T. Greber, B. Buchner and A. A. Popov, Methane as a Selectivity Booster in the Arc-Discharge Synthesis of Endohedral Fullerenes: Selective Synthesis of the Single-Molecule Magnet Dy2TiC@C80 and Its Congener Dy<sub>2</sub>TiC<sub>2</sub>@C<sub>80</sub>, Angew. Chem., Int. Ed., 2015, 54, 13411-13415.
- 34 M. N. Chaur, R. Valencia, A. Rodriguez-Fortea, J. M. Poblet and L. Echegoyen, Trimetallic Nitride Endohedral Fullerenes: Experimental and Theoretical Evidence for the  $M_3N^{6+}$   $(3C_{2n}^{(6-)})$  model, Angew. Chem., Int. Ed., 2009, 48, 1425-1428.
- 35 J. M. Campanera, C. Bo and J. M. Poblet, General rule for the stabilization of fullerene cages encapsulating trimetallic nitride templates, Angew. Chem., Int. Ed., 2005, 44, 7230-7233.
- 36 A. A. Popov and L. Dunsch, Structure, stability, and clustercage interactions in nitride clusterfullerenes M3N@C2n (M = Sc, Y; 2n = 68-98): a density functional theory study, J. Am. Chem. Soc., 2007, 129, 11835-11849.
- 37 Y. Hu, Y.-R. Yao, X. Liu, A. Yu, X. Xie, L. Abella, A. Rodriguez-Fortea, J. M. Poblet, T. Akasaka, P. Peng, Q. Zhang, S.-Y. Xie, F.-F. Li and X. Lu, Unexpected formation of 1,2- and 1,4-bismethoxyl Sc<sub>3</sub>N@I<sub>h</sub>,-C<sub>80</sub> derivatives via regioselective anion addition: an unambiguous structural identification and mechanism study, Chem. Sci., 2021, 12, 8268-8268.
- 38 F. Jin, J. Xin, R. Guan, X. Xie, M. Chen, Q. Zhang, A. A. Popov, S.-Y. Xie and S. Yang, Stabilizing a three-center single-electron metal-metal bond in a fullerene cage, Chem. Sci., 2021, 12, 6890-6895.
- 39 Y.-Y. Xu, H.-R. Tian, S.-H. Li, Z.-C. Chen, Y.-R. Yao, S.-S. Wang, X. Zhang, Z.-Z. Zhu, S.-L. Deng, Q. Zhang, S. Yang, S.-Y. Xie, R.-B. Huang and L.-S. Zheng, Flexible decapyrrylcorannulene hosts, Nat. Commun., 2019, 10, 485.
- 40 H. Kurihara, X. Lu, Y. Iiduka, H. Nikawa, N. Mizorogi, Z. Slanina, T. Tsuchiya, S. Nagase and T. Akasaka, Chemical Understanding of Carbide Cluster Metallofullerenes: A Case Study on  $Sc_2C_2@C_{2\nu}(5)$ - $C_{80}$  with Complete X-ray Crystallographic Characterizations, J. Am. Chem. Soc., 2012, 134, 3139-3144.
- 41 X. Liu, B. Li, W. Yang, Y.-R. Yao, L. Yang, J. Zhuang, X. Li, P. Jin and N. Chen, Synthesis and characterization of carbene derivatives of Th@ $C_{3v}(8)$ -C<sub>82</sub> and U@ $C_{2v}(9)$ -C<sub>82</sub>: exceptional chemical properties induced by strong actinide-carbon cage interaction, Chem. Sci., 2021, 12, 2488-2497.
- 42 W. Zhang, M. Suzuki, Y. Xie, L. Bao, W. Cai, Z. Slanina, S. Nagase, M. Xu, T. Akasaka and X. Lu, Molecular

- Structure and Chemical Property of a Divalent Metallofullerene Yb@ $C_2(13)$ - $C_{84}$ , *J. Am. Chem. Soc.*, 2013, 135, 12730–12735.
- 43 X. Lu, H. Nikawa, L. Feng, T. Tsuchiya, Y. Maeda, T. Akasaka, N. Mizorogi, Z. Slanina and S. Nagase, Location of the yttrium atom in Y@C<sub>82</sub> and its influence on the reactivity of cage carbons, *J. Am. Chem. Soc.*, 2009, 131, 12066–12067.
- 44 C. Chen, F. Liu, S. Li, N. Wang, A. A. Popov, M. Jiao, T. Wei, Q. Li, L. Dunsch and S. Yang, Titanium/Yttrium Mixed Metal Nitride Clusterfullerene TiY<sub>2</sub>N@C<sub>80</sub>: Synthesis, Isolation, and Effect of the Group-III Metal, *Inorg. Chem.*, 2012, 51, 3039–3045.
- 45 S. Wang, J. Huang, C. Gao, F. Jin, Q. Li, S.-Y. Xie and S. Yang, Singly Bonded Monoadduct rather than Methanofullerene: Manipulating the Addition Pattern of Trimetallic Nitride Clusterfullerene through One Endohedral Metal Atom Substitution, *Chem. Eur. J.*, 2016, 22, 8309–8315.
- 46 G. M. Sheldrick, Crystal structure refinement with SHELXL, *Acta Crystallogr., Sect. C: Struct. Chem.*, 2015, **71**, 3–8.
- 47 O. V. Dolomanov, L. J. Bourhis, R. J. Gildea, J. A. Howard and H. Puschmann, OLEX2: a complete structure solution, refinement and analysis program, *J. Appl. Crystallogr.*, 2009, 42, 339–341.